ASTRONOMY & ASTROPHYSICS
SUPPLEMENT SERIES

Astron. Astrophys. Suppl. Ser. **129,** 329-336 (1998)

A deep λ20 cm radio continuum survey of M 31

R. Beck, E.M. Berkhuijsen, and P. Hoernes

Max-Planck-Institut für Radioastronomie, Auf dem Hügel 69, D-53121 Bonn, Germany

Received December 12, 1996; accepted September 29, 1997

Abstract. We present a survey of the total and linearly polarized radio continuum emission of the Andromeda galaxy at 20 cm wavelength with the VLA-D array. 7 fields were observed with 45″ angular resolution. The missing large-scale total emission observed with the Effelsberg telescope was inserted. This survey is the most sensitive radio continuum survey of M 31 so far and the first one in linear polarization with the VLA.

The total emission of M 31 comes from extended regions and point sources. Both components are concentrated in the bright "ring" of maximum star formation at about 10 kpc radius. Nearly half of the extended emission emerges from numerous filamentary features which are typically a few arcminutes long ($\simeq$ 600 pc). In the field of M 31, 36 linearly polarized background sources were detected.

The smallest degrees of polarization occur on the centre of the "ring" where the total emission is highest, hence on the spiral arms as delineated by Hα emission and OB associations. The distribution of polarization angles reveals coherent features of typically 1 kpc in extent, some of which show a relation to an OB association.

Key words: techniques: interferometric — galaxies: individual: M 31 — galaxies: magnetic fields — radio continuum: galaxies — polarization

1. Introduction

M 31 – the Andromeda Galaxy – is the nearest spiral galaxy on the sky and it was the first external galaxy detected in radio continuum (Hanbury Brown & Hazard 1950). Surveys with the Effelsberg telescope and with the Cambridge and Westerbork synthesis instruments revealed a ring-like structure at about 10 kpc radius (Pooley 1969; Berkhuijsen & Wielebinski 1974; Beck & Gräve 1982) and a large number of point-like sources (Bystedt et al. 1984; Walterbos et al. 1985). The northern half of M 31 was mapped with the VLA by Braun (1990) who detected some extended emission at a resolution of 90″ using a special code to account for the missing spacings.

Polarized radio emission from M 31 was first detected by Beck et al. (1978, 1980) with the Effelsberg 100-m telescope at λ11 cm. The magnetic field structure can be modeled by a torus of field lines with uniform direction without radial reversals (Beck 1982; Ruzmaikin et al. 1990) consistent with dynamo theory (Poezd et al. 1993). However, these results were based on modeling the distribution of polarization angles and polarized intensity at only one wavelength.

In an Effelsberg survey at λ6 cm significant polarized emission was detected in the bright "ring" within 30′ of the minor axis and within 5′ south of the centre (Berkhuijsen et al. 1987). Together with VLA observations at λ20 cm of a region in the "ring" southwest of the centre the torus model of the magnetic field was basically confirmed, but in the "ring" also periodical field structures on smaller spatial scales were discovered (Beck et al. 1989).

This paper presents a complete VLA survey of M 31 at λ20 cm of the total emission and, for the first time, the linearly polarized emission, combined with low-resolution observations of the total emission with the Effelsberg telescope at the same wavelength.

2. Observations and data reduction

2.1. The VLA maps

The 10-kpc "ring" of M 31 has an angular diameter along the major axis of $\simeq 1\overset{\circ}{.}7$ while the beamsize of a single VLA telescope (the primary beam) at λ20 cm is only $0\overset{\circ}{.}5$. To cover the whole area, observations of 7 fields ("pointings") with the VLA-D array were collected during 9 years (Table 1). The angular resolution is 45″. As the upgrade of the *L*-band systems took place between 1990 and 1993, only the last 3 pointings could profit from the improved sensitivity. Unfortunately, at the same time the interference situation became worse so that the second IF at 1515 MHz could not be used anymore. The rms noise in the final maps varies between the different pointings due to different observation times, different system

Table 1. VLA observations

Field	Coordinates of phase centre RA (1950.0) [h m s]	DEC (1950.0) [° ′ ″]	Centre frequencies [MHz] IF 1/2	Date	Effective observation time [h] IF 1/2	Rms noise in final TP map [μJy/beam]	Rms noise in final Q, U maps [μJy/beam]
1 (C)	00 37 30	40 30 00	1465/1515	1987 Apr. 13	8.0/7.6	50	30
2 (A)	00 38 36	40 54 00	1465/1515	1983 July 15	4.1/4.8	45	30
3 (B)	00 39 22	40 34 00	1465/1515	1988 Sept. 8	8.3/5.6	45	25
4 (D)*	00 40 01.8	40 59 46	1465/1515	1989 Dec. 20	4.4/4.4	60	25
5 (E)	00 40 21	41 25 00	1465/–	1992 July 25+27	6.1/–	85	30
6 (F)	00 42 05	41 10 00	1465/–	1992 July 25+27	6.2/–	50	20
7 (G)	00 42 23	41 35 00	1465/–	1992 July 25+27	6.1/–	50	25

*centre.

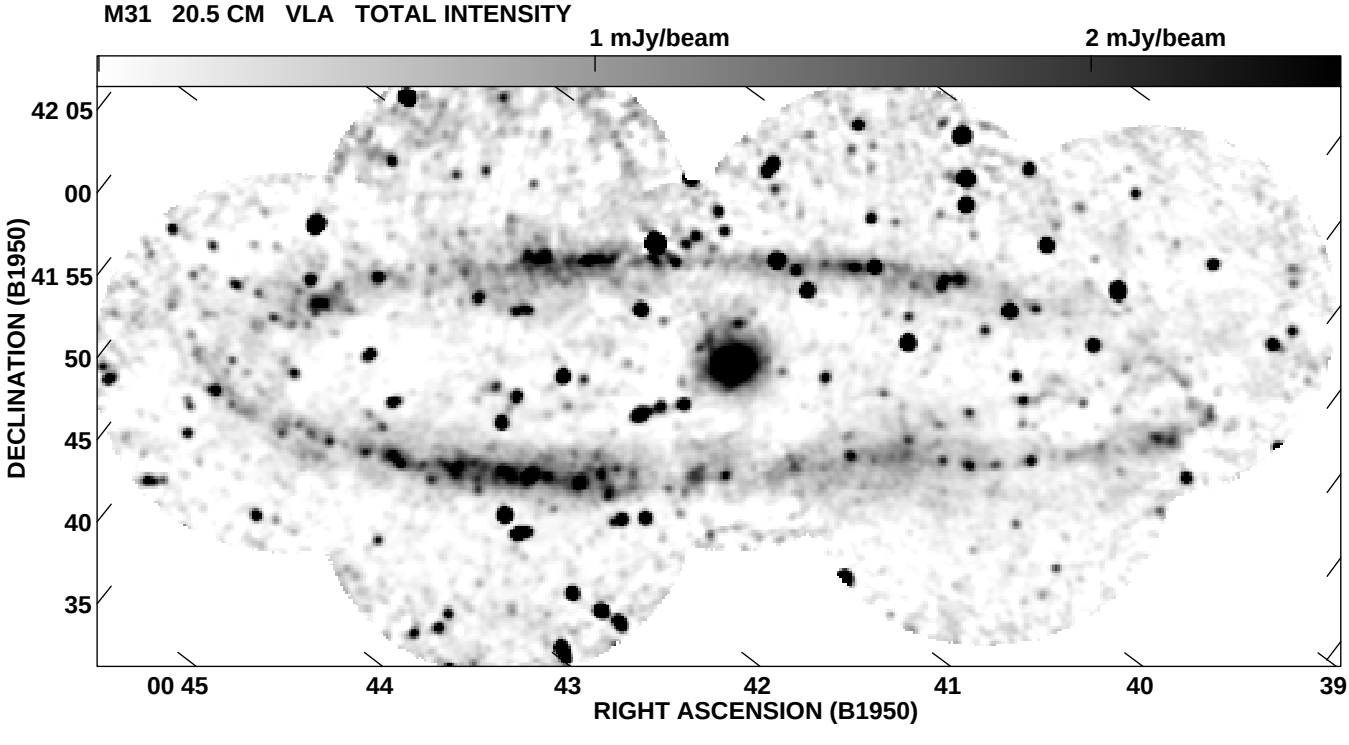

Fig. 1. Mosaic of 7 fields on M 31 showing the total power emission at λ20.5 cm observed with the VLA-D array. The angular resolution is 45″. The rms noise generally is ≃ 75 μJy/beam increasing to ≃ 150 μJy/beam at the borders of the map

sensitivities and a different amount of data affected by interference. In linear polarization, the rms noise is almost the same for all pointings.

All data were reduced at the MPIfR Bonn using the standard AIPS package. 3C 48 and 3C 138 were used for absolute flux density and polarization angle calibration, 0038+328 for gain and phase calibration. Self-calibration was performed on each field individually using the AIPS task ASCAL. Comparison of the total flux densities of unresolved background sources in overlapping regions of two (or more) fields yielded good consistency within a few percent, except for field A (the first one observed). Here all flux densities were found to be higher by 9%, for which the maps in Stokes parameters I(total intensity), Q and U were corrected.

For each Stokes parameter the maps of all fields were combined by applying the AIPS task LPTES which is similar to the standard LTESS, but cuts the individual maps

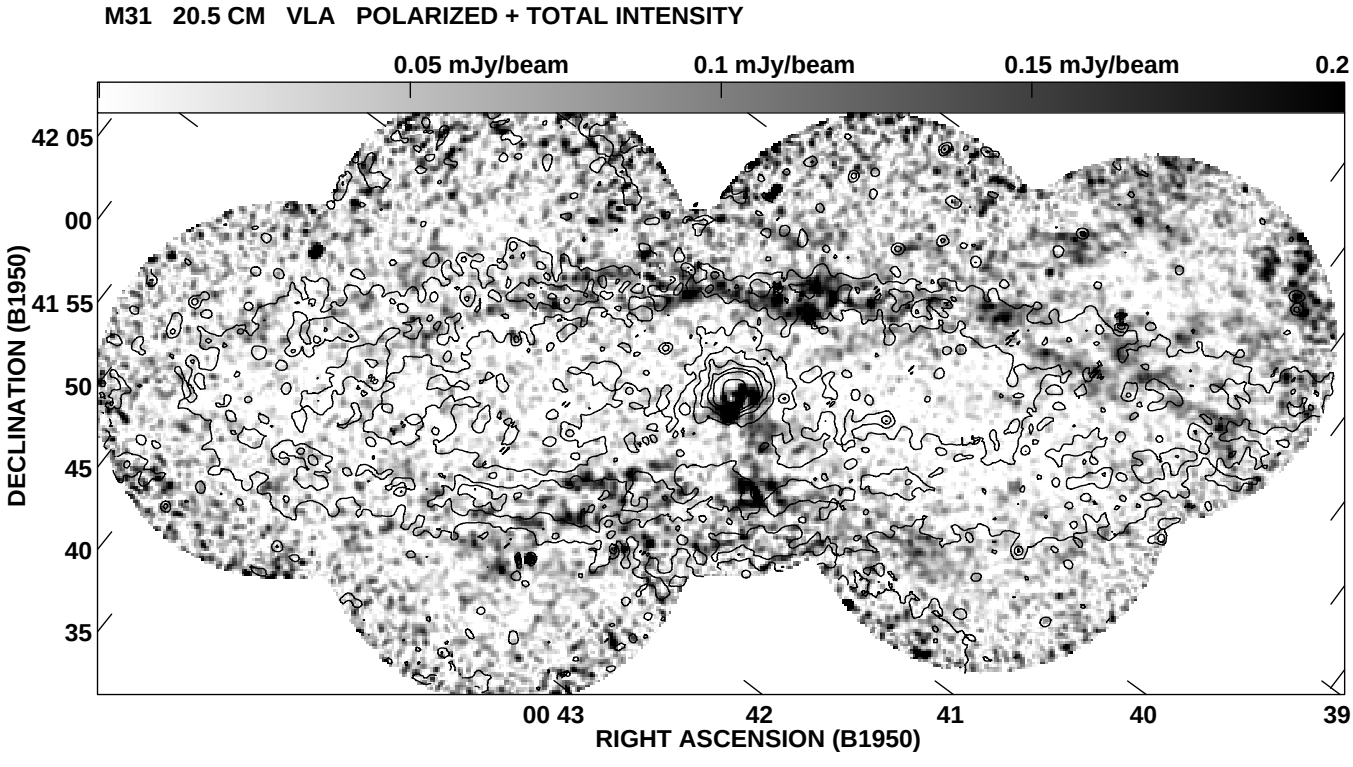

Fig. 2. Mosaic of 7 fields on M 31 showing the linearly polarized emission at λ20.5 cm observed with the VLA-D array. The angular resolution is 45″. The rms noise generally is ≃ 25 μJy/beam increasing to ≃ 50 μJy/beam at the borders of the map. Point sources brighter than 1 mJy in polarized intensity are subtracted. The position of the bright "ring" is shown by contours of the total emission (see Fig. 4). The contour levels are 0.6, 1.2, 1.8, 2.4, 3.0 and 6.0 mJy/beam

at a chosen radius from the field centre. We chose a radius where the sensitivity is down to 30% in order to avoid a large increase of the noise level at the edges of the combined map. The combined maps in Stokes Q and U were transformed into maps of the polarization angle and of the polarized intensity by taking $(Q^2 + U^2)^{1/2} - 1.3\sigma_{Q,U}$ where $\sigma_{Q,U} = 30\,\mu$Jy/beam (Wardle & Kronberg 1974).

The resulting maps in total and linearly polarized intensities are shown in Figs. 1 and 2, respectively. The rms noise within the main regions of M 31 is ≃ 75 μJy/beam in total power and ≃ 25 μJy/beam in polarized intensity, increasing to about twice these values at the singly-covered map edges. Hence these maps represent the most sensitive radio continuum survey of M 31 so far and the first one in linear polarization with the VLA.

2.2. The Effelsberg map

The largest structure visible to the VLA-D array at λ20.5 cm is ≃ 15′ due to the lack of short interferometer spacings. To fill these short spacings, observations at 1400 MHz (λ21.4 cm) were performed with the 100-m Effelsberg telescope of the MPIfR between 1993 and 1995. The bandwidth used was 20 MHz. The system temperature was 26 K and the angular resolution 9′.35. A field of 5° × 5° in M 31 coordinates (37° position angle of the major axis) was scanned 2 times in λ- and 3 times in β-direction, yielding a noise level of 5 mJy/beam. The scanning effects were removed by a weighted addition of the maps with different scanning angles in the Fourier plane (see Emerson & Gräve (1988) for explanation of the algorithm).

M 31 is located on a spur of Galactic radio continuum emission (Gräve et al. 1981). Subtraction of this foreground emission in total intensity was achieved by a careful application of the BGF algorithm (Sofue & Reich 1979) after subtraction of known background point sources.

The final map in total intensity is shown in Fig. 3. Unfortunately, at this low angular resolution the polarized emission from M 31 cannot be separated from that from the Galactic foreground.

3. Combination of the VLA and Effelsberg maps

The combination of the Effelsberg total-intensity map with the mosaic of VLA maps was carried out using the program EFFMERG, a modified version of the SDE task IMERG (Cornwell et al. 1995). IMERG deconvolves each of the two maps with its beam, adds them in the Fourier domain, using the Effelsberg data for small spacings, VLA

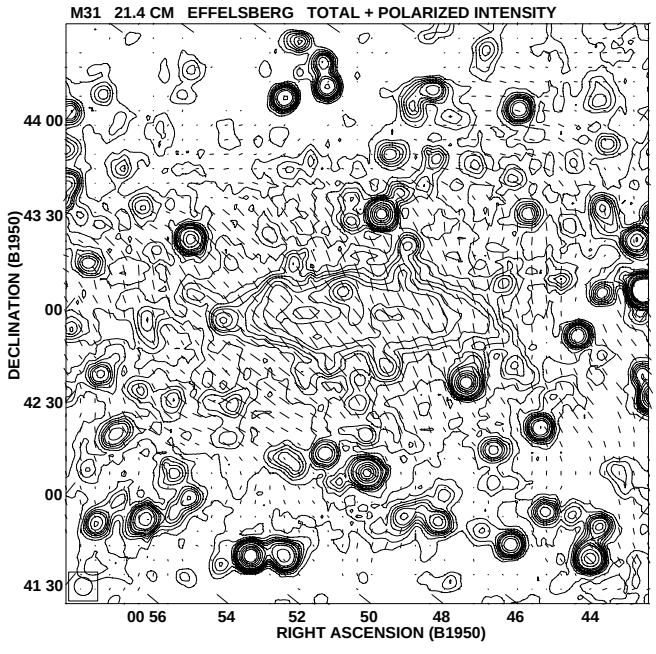

Fig. 3. Total emission (contours) and E-vectors of the polarized emission at λ21.4 cm of a $5^\circ \times 5^\circ$ field containing M 31 observed with the 100-m Effelsberg telescope. The angular resolution is $9'.35$. The rms noise is about 5 mJy/beam. Contour levels are 20, 40, ..., 100, 160, 200, 300, ..., 600 mJy/beam. The maximum polarized intensity of 121 mJy/beam corresponds to a vector plotted with $11'$ length

data for large spacings and a linear interpolation in the overlap domain, and finally convolves the combined map with the VLA beam. The only free parameters are the maximum spacing of the Effelsberg map and the minimum spacing of the VLA map (both in units of λ).

The results for extended emission are generally satisfying, but ring-like distortions around point sources limit the dynamic range in the combined map to about 2000 times the rms noise. The performance of this algorithm was demonstrated before (Beck & Hoernes 1996). We did not apply combination tasks based on MEM like VTESS in AIPS because this does not deconvolve the beams. Test runs were unsatisfactory; future improved MEM routines are required.

In the case of M 31 several difficulties had to be overcome. In order to get a combined map with flat baselines and without distortions, we first had to subtract strong point-like sources from the VLA map. The subtracted sources were smoothed to the Effelsberg resolution and subtracted from the Effelsberg map. Then the residual single-dish map was smoothed to a resolution of about $15'$ in order to weaken the influence of source residuals. This still guarantees full coverage of the UV plane after application of EFFMERG, thus avoiding baseline problems around the residuals of strong background sources. This map was then combined with the residual VLA map by EFFMERG, using a maximum spacing of 250λ for the Effelsberg map and a minimum spacing of 190λ for the VLA map. After combination, the VLA point sources were added again.

The combined map of total intensities but without point-like sources (see Sect. 4.1) is shown in Fig. 4.

In polarized intensity, the combination of Effelsberg and VLA maps was impossible due to the strong foreground polarization.

4. Results

4.1. Point-like sources

Our maps of total intensities (Figs. 1 and 3) show a large number of unresolved (point-like) sources. As most of these have been catalogued before (Walterbos et al. 1985; Braun 1990), we do not give a new source list in this paper[1]. Differences in flux density may result from the different telescope beams or from source variability. With the larger beam of our survey, we find significantly larger flux densities for 37W45, 50, 51, 175, 180, 201, 207A and 207B. Except for 37W207 these sources were classified as extended by Walterbos et al. (1985). Lower flux densities (possibly due to variability) are found for the sources 37W91, 115, 131, 168 and 200.

As this is the first M 31 survey at λ20 cm including linearly polarized emission, we give a list of polarized sources in Table 2. These sources may be used e.g. to search for systematic variations of Faraday rotation in the disk and halo of M 31.

Many of the unpolarized sources seen on M 31 are H II regions or weak supernova remnants. In the northern half of M 31 Braun (1990) identified 103 H II regions and Braun & Walterbos (1993) detected 52 SNRs and SNR candidates.

In order to obtain a map of M 31 largely free of unrelated point sources we subtracted all sources brighter than 2 mJy. As 25% of the identified H II regions and 10% of the SNRs and SNR candidates are brighter than 2 mJy, this means that the brightest H II regions and SNRs were also subtracted. The resulting combined map of total intensities is shown in Fig. 4.

4.2. Integrated flux density and extended total emission

After subtraction of unresolved sources brighter than 2 mJy we integrated the flux densities of our VLA maps (Figs. 1 and 2) in ellipses around the centre out to a radius of 16 kpc in the plane of the galaxy (inclined by 78°). The total flux density is 1.73 ± 0.22 Jy in total intensity and 0.31 ± 0.10 Jy in linear polarization. The combined map in total intensity (Fig. 4) includes 3.76 ± 0.40 Jy within the same radius. This demonstrates the significance of the

[1] A digital version of the source list can be obtained from the authors.

Table 2. Polarized point-like sources in the M 31 field

Name 37W	α_{1950} (00^h) [m s]	δ_{1950} [° ′ ″]	S_p [μJy]	S [μJy]	p [%]	χ [°]
31	36 43.8	40 37 59	220±30	3790± 50	5.8±0.8	30±4
36	36 49.7	40 27 37	340±60	8680± 50	3.9±0.7	52±5
45	37 13.2	40 55 11	4580±50	60390±170	7.6±0.9	70.9±0.3
51	37 30.1	40 33 39	290±30	39680±320	0.7±0.1	29±3
50	37 30.1	40 52 18	2890±40	38620±190	7.5±0.1	157.7±0.4
52	37 33.2	40 41 59	600±30	21280± 60	2.8±0.2	104±2
57	37 41.1	40 50 46	1430±30	28470±100	5.0±0.1	77.5±0.6
74A	38 23.8	41 08 29	860±70	10170±100	8.5±0.7	152±2
76	38 27.6	40 17 04	210±40	4840± 60	4.3±0.8	74±6
74B	38 28.9	41 08 31	1310±80	7320± 90	17.9±1.1	97±2
82	38 37.9	40 36 35	150±40	4410± 50	3.4±0.9	49±8
—	38 50.1	41 30 12	290±50	1800±110	16.1±2.9	114±5
91	38 57.3	40 47 09	2120±30	46300±120	4.6±0.1	120.3±0.4
94	39 03.8	41 02 22	780±50	41560±120	1.9±0.1	75±2
95	39 07.0	40 58 11	390±30	22960± 70	1.7±0.1	74±2
115	39 34.7	41 13 01	5770±60	306940±650	1.9±0.1	41.0±0.3
127	39 46.1	40 21 55	190±40	1970± 50	9.6±2.0	80±6
131	39 51.2	41 41 17	2390±70	61590±180	3.9±0.1	174.1±0.8
144	40 07.4	41 10 10	660±30	21800± 70	3.0±0.1	21±1.3
152	40 23.1	41 38 42	500±40	4080± 80	12.3±1.0	168±2
168	40 56.6	40 38 03	1990±50	52090±340	3.8±0.1	124.9±0.7
169	41 00.2	41 12 19	680±30	21130±110	3.2±0.2	73±1.3
175	41 14.3	41 40 51	990±50	76940±190	1.3±0.1	111±1.4
180	41 23.3	41 14 45	320±60	6710± 50	4.8±0.9	100±5
185	41 33.8	40 57 17	240±30	11390± 50	2.1±0.3	114±4
188	41 39.3	41 14 19	1230±30	12600± 50	9.8±0.2	111.1±0.7
190	41 41.8	40 59 03	250±60	8740± 80	2.9±0.7	127±7
200	42 02.4	41 51 50	260±60	3840± 80	6.8±1.6	151±7
201	42 05.0	41 24 03	150±40	5570± 60	2.7±0.7	68±8
205	42 17.0	41 08 30	1040±30	42820±100	2.4±0.1	22.6±0.8
207A	42 17.7	41 05 48	430±60	8150±110	5.3±0.8	63±4
207B	42 21.0	41 06 22	1340±70	16050±120	8.3±0.5	127±2
211	42 26.9	40 55 08	3580±50	28540±130	12.5±0.2	154.6±0.4
219	42 54.9	40 55 59	520±50	27950±160	1.9±0.2	170±3
—	42 57.6	40 55 06	460±60	8080±180	5.7±0.8	12±4
—	43 26.4	41 47 45	190±40	5470±200	3.5±0.8	155±6

Name: source number in Walterbos et al. (1985); S_p: linearly polarized flux density; S: total flux density; p: degree of polarization; χ: polarization angle.

effect of missing interferometer spacings in the case of an extended object like M 31.

To the total flux density at λ20 cm derived here we should add about 300 mJy of subtracted H II regions and SNRs in M 31 brighter than 2 mJy. The value of 4.1 ± 0.5 Jy then is in good agreement with that expected from the spectrum between λ74 cm and λ11 cm (Beck & Gräve 1982), 4.21 ± 0.24 Jy. We note, however, that our value at λ20 cm is a lower limit as along the major axis the combined map extends only to 12 kpc radius (compared to 16 kpc at λ11 cm).

Our Effelsberg map (Fig. 3) shows the full extent of M 31. After subtraction of the Galactic foreground emission and of the unresolved background sources (visible in our VLA map) we obtained a total flux density of 4.6 ± 0.4 Jy within 16 kpc radius.

The extended total emission seen in the VLA map (Fig. 1) emerges from many small-scale features which often seem filamentary. These filamentary structures are seen in the "ring", i.e. around the spiral arms and in interarm regions, and are typically about 3′ (= 600 pc) long. The contribution of the filamentary emission to the total

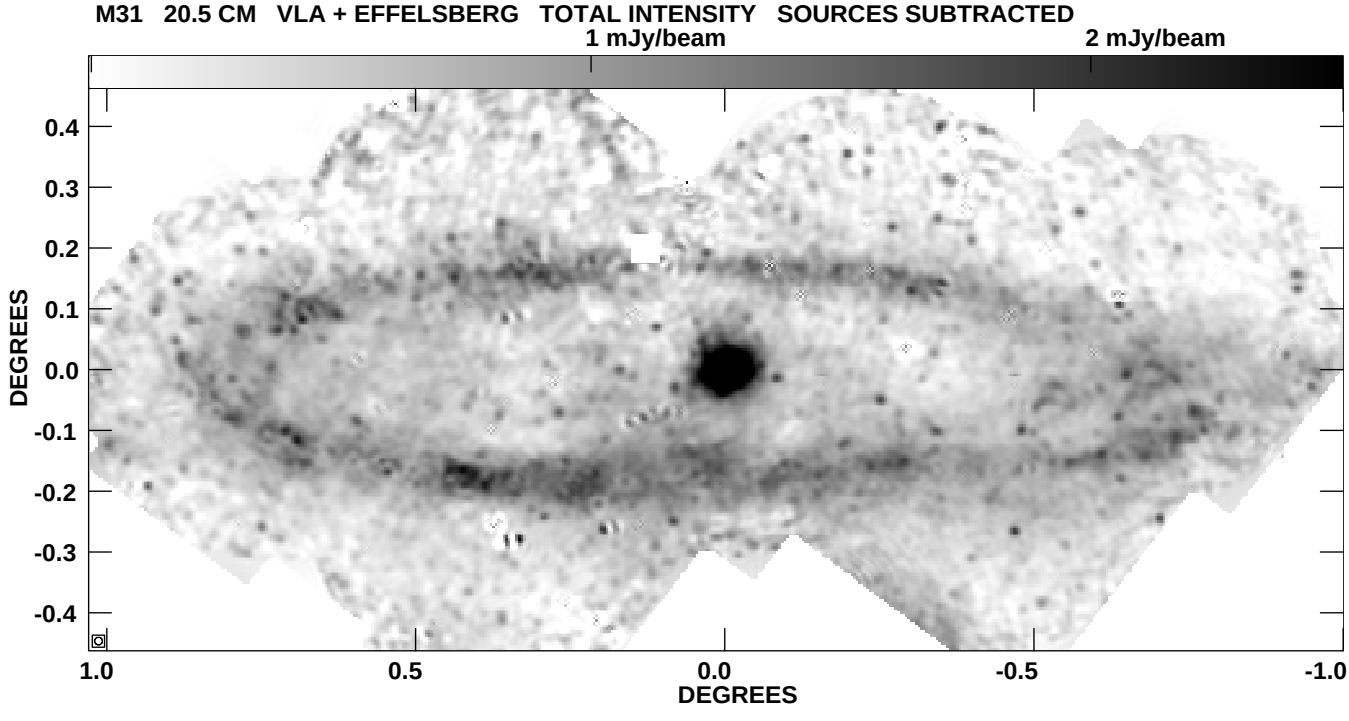

Fig. 4. Total emission of M 31 at λ20 cm observed with the VLA-D array (Fig. 1) combined with that observed with the Effelsberg telescope (Fig. 3) to correct for the missing interferometer spacings. The angular resolution is 45″. The rms noise generally is $\simeq 75\,\mu$Jy/beam increasing to $\simeq 150\,\mu$Jy/beam at the map edges. All point sources brighter than 2 mJy are subtracted. Blank squares indicate regions where subtraction of Gaussian profiles was insufficient. The coordinate system is centred on M 31 ($\alpha_{50} = 0^{\rm h}40^{\rm m}1\overset{\rm s}{.}8$, $\delta_{50} = +40^\circ59'46''$, position angle of major axis = 37°)

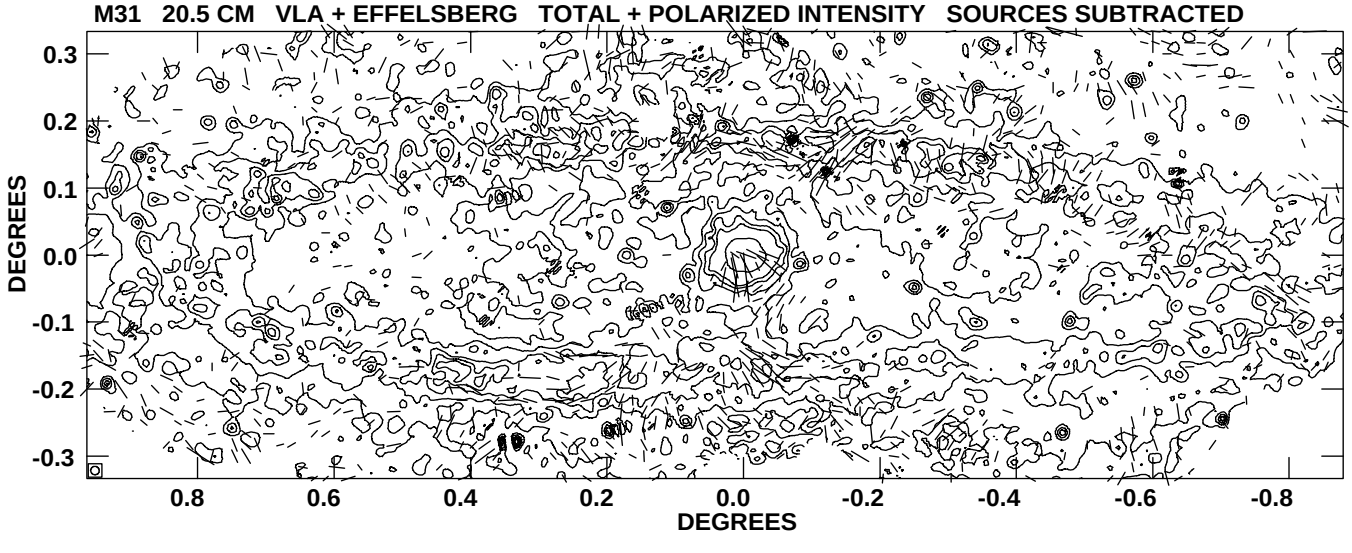

Fig. 5. Combined VLA–Effelsberg map of the total emission of M 31 at λ20 cm with E-vectors of polarized emission (VLA only) superimposed. The contour levels are 0.4, 0.8, 1.2, 1.6, 2.0 and 4.0 mJy/beam. The angular resolution is 45″. Point sources brighter than 2 mJy are subtracted. A vector plotted with 1′ length corresponds to a polarized intensity of 100 μJy/beam. As in Fig. 4 the coordinate system is centred on M 31

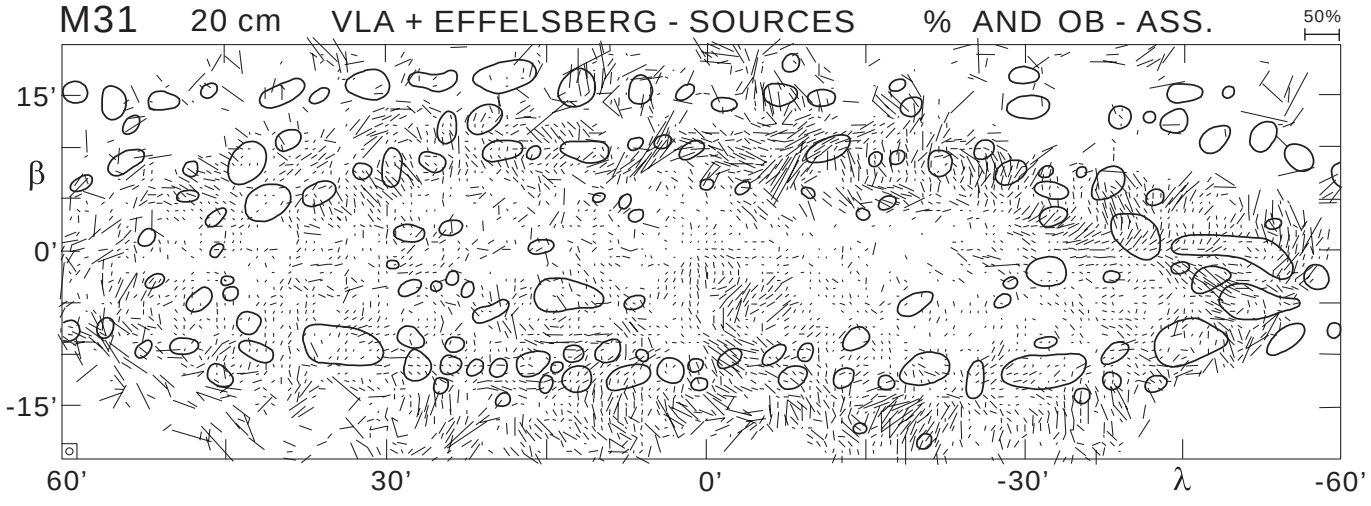

Fig. 6. Distribution of the degree of polarization in M 31 (vectors) with positions of OB associations catalogued by van den Bergh (1964) (ellipses) superimposed. Cells of coherent polarization angles are clearly visible. For the coordinate system centred on M 31 a position angle of the major axis of 37° was used. No corrections for Faraday rotation were applied

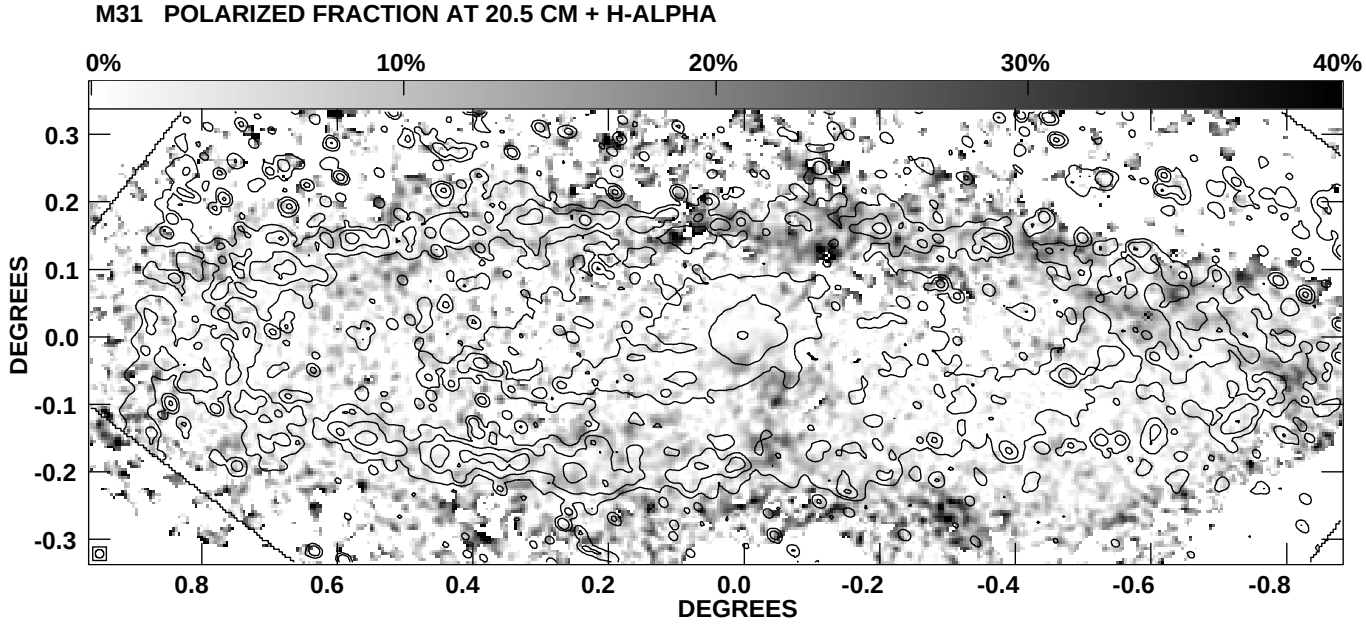

Fig. 7. Distribution of the degree of polarization in M 31 shown in grey-scale with contours of the surface brightness in Hα (Devereux et al. 1994) superimposed, smoothed to a beam size of 45″. The contour levels are 0.5, 1.5, 5 and 25 in units of 1.947 10^{-14} erg s^{-1} cm^{-2} beam^{-1}. The M 31 coordinates are based on a position angle of the major axis of 37°

extended emission seen in Fig. 4 may be estimated from the total flux densities given above as $\lesssim 40\%$.

4.3. Foreground polarization

We checked our M 31 field for polarized features in the Galactic foreground of the kind discovered by Wieringa et al. (1993) with the WSRT. At 327 MHz these authors detected polarized filaments, typically 4′ wide and up to 1° long, which are not visible in the total emission. They interpreted these features as modulations of a smooth polarized Galactic background by filaments in an ionized foreground. The filaments are generally parallel to the Galactic plane.

In Fig. 5 we show the polarization E-vectors (VLA only) on a contour map of the total (VLA+Effelsberg) emission. Neither in this figure nor in Fig. 2 we see filaments of the kind observed by Wieringa et al. running across M 31 parallel to the Galactic plane (which is practically parallel to constant declination in these

figures). The absence of polarized foreground filaments in our maps at 1465 MHz is consistent with the experience of Wieringa et al. that the filaments are not visible at 610 MHz or 1420 MHz.

4.4. The polarized emission

The polarized emission of M 31 shown in Figs. 2 and 5 is clearly concentrated in the area of the bright "ring" seen in total power. Out to 12 kpc radius the average degree of polarization is $6.6 \pm 2.1\%$ (see Sect. 4.2). This value is a lower limit because large-scale polarized emission from M 31 is missing in Figs. 2 and 5. However, small-scale variations in the degree of polarization can still be studied.

The highest polarized intensities occur not on the centre of the "ring" but on the inner and outer edges, giving the impression of filaments. This phenomenon is most clearly visible in Fig. 2 at about $20'$ on either side of the minor axis. Many polarized filaments exist on scales of about $1' \times 3'$ to $10'$ running preferentially along the spiral arms.

The same effect is visible in the distribution of the percentage polarization shown in Fig. 6, on which the positions of the OB associations (van den Bergh 1964) are superimposed. On the spiral arms as delineated by the OB associations the degree of polarization is generally low, but across the arms it increases towards the interarm regions. Relatively low degrees of polarization on spiral arms also occur in other galaxies (Beck et al. 1996) and are due to Faraday effects and turbulence in the interstellar medium in the arms causing depolarization. The very low degrees of polarization inside some OB associations in Fig. 6 support this interpretation.

In Fig. 6 the polarization angles of the electric vector seem rather chaotic. Closer inspection, though, reveals cells of coherent polarization angles of $3'$– $7'$ in extent corresponding to about 1 kpc in the plane of M 31. A sudden change of polarization angles often occurs near the border of an OB association suggesting that supernova remnants in the association deform the regular magnetic field causing variations in Faraday rotation. Brinks & Bajaja (1986) showed that many OB associations are surrounded by an H I hole which needs $10^{49} - 10^{53}$ erg to be produced. The largest H I holes have diameters of $\sim$ 1 kpc and thus mean energy densities of $\sim 10^{-12}\,\mathrm{erg\,cm^{-3}}$, enough to deform magnetic fields of $\sim 5\,\mu$G strength.

Figure 7 shows the distribution of the percentage polarization in grey-scale with contours of surface brightness in Hα (Devereux et al. 1994) superimposed. Especially in the northern part of the bright "ring" a clear anticorrelation between degree of polarization and Hα intensity exists, but like with the OB associations there is little one-to-one correlation. As apart from the density of thermal electrons other factors are involved in depolarization (Sokoloff et al. 1998), this is understandable.

Detailed discussions of the distribution of rotation measure and of depolarization across M 31 derived from data at λ20 cm (this paper), λ11 cm (Beck 1982) and the new Effelsberg survey at λ6 cm (Beck et al. in preparation) will be given in forthcoming papers.

Acknowledgements. We wish to thank Dr. E. Hummel and Dr. A.P. Rao for assistence in the data reduction, Dr. N. Devereux for putting the Hα-map at our disposal, and the referee Dr. S. Sukumar for useful comments on the manuscript. The VLA staff is acknowledged for help in preparing the observations and for performing them.

References

Beck R., 1982, A&A 106, 121
Beck R., Gräve R., 1982, A&A 105, 192
Beck R., Hoernes P., 1996, Nat 379, 47
Beck R., Berkhuijsen E.M., Wielebinski R., 1978, A&A 68, L27
Beck R., Berkhuijsen E.M., Wielebinski R., 1980, Nat 283, 272
Beck R., Brandenburg A., Moss D., Shukurov A., Sokoloff D., 1996, ARA&A 34, 153
Beck R., Loiseau N., Hummel E., et al., 1989, A&A 222, 58
Berkhuijsen E.M., Wielebinski R., 1974, A&A 34, 173
Berkhuijsen E.M., Beck R., Gräve R., 1987, in: Beck R., Gräve R. (eds.) Interstellar Magnetic Fields. Springer, Berlin, p. 38
Berkhuijsen E.M., Bajaja E., Beck R., 1993, A&A 279, 359
Braun R., 1990, ApJS 72, 761
Braun R., 1991, ApJ 372, 54
Brinks E., Bajaja E., 1986, A&A 169, 14
Bystedt J.E.V., Brinks E., de Bruyn A.G., et al., 1984, A&AS 56, 245
Cornwell T.J., Briggs D.S., Holdaway M.A., 1995, User's Guide to SDE. NRAO, Socorro
Devereux N.A., Price R., Wells L.A., Duric N., 1994, AJ 108, 1667
Emerson D.T., Gräve R., 1988, A&A 190, 353
Gräve R., Emerson D.T., Wielebinski R., 1981, A&A 98, 260
Hanbury Brown R., Hazard C., 1950, Nat 166, 901
Poezd A., Shukurov A., Sokoloff D., 1993, MNRAS 264, 285
Pooley G.G., 1969, MNRAS 144, 101
Ruzmaikin A., Sokoloff D., Shukurov A., Beck R., 1990, A&A 230, 284
Sofue Y., Reich W., 1979, A&AS 38, 251
Sokoloff D.D., Bykov A.A., Shukurov A., et al., 1998, MNRAS (submitted)
van den Bergh S., 1964, ApJS 86, 65
Walterbos R.A.M., Brinks E., Shane W.W., 1985, A&AS 61, 451
Wardle J.F.C., Kronberg P.P., 1974, ApJ 194, 249
Wieringa M.H., de Bruyn A.G., Jansen D., Brouw W.N., Katgert P., 1993, A&A 268, 215